Published in final edited form as:
Neuroscience. 2013 March 13; 233: 54–63. doi:10.1016/j.neuroscience.2012.12.025.

DENDRITIC SPINE ALTERATIONS IN THE HIPPOCAMPUS AND PARIETAL CORTEX OF ALPHA7 NICOTINIC ACETYLCHOLINE RECEPTOR KNOCKOUT MICE

B. J. Morley[a,*] and **R. F. Mervis**[b,c]

[a]Boys Town National Research Hospital, 555 North 30th Street, Omaha, NE 68131, United States

[b]Center for Aging and Brain Repair, Department of Neurosurgery and Brain Repair, University of South Florida Morsani College of Medicine, Tampa, FL 33612, United States

[c]NeuroStructural Research Laboratories, Inc., 12409 Telecom Drive, Tampa, FL 33612, United States

Abstract

The α7 nicotinic acetylcholine receptor (nAChR) is involved in higher cognitive and memory functions, and is associated with the etiology of neurological diseases involving cognitive decline, including Alzheimer's disease (AD). We hypothesized that spine changes in the α7 knockout might help to explain the behavioral deficits observed in α7 knockout mice and prodromal hippocampal changes in AD. We quantified several measures of dendritic morphology in the CA1 region of the mouse hippocampus in Golgi-stained material from wildtype and α7 knockout mice at P24. The most significant difference was a 64% increase in thin (L-type) dendritic spines on the CA1 basilar tree in knockout mice ($p < .05$). There were small decreases in the number of in N-type (−15%), M-type (−14%) and D-type (−4%) spine densities. The CA1 basilar dendritic tree of knockout mice had significantly less branching in the regions nearthesoma in comparison with wildtype animals ($p < .01$), but not in the more distal branching. Changes in the configuration of CA1 basilar dendritic spines have been observed in a number of experimental paradigms, suggesting that basilar dendritic spines are highly plastic. One component of cognitive dysfunction may be through α7-modulated GABAergic interneurons synapsing on CA1 basal dendrites.

Keywords

alpha7 nicotinic receptor; hippocampus; dendrite; CA1 region; parietal cortex; cognition

INTRODUCTION

Neural networks containing nicotinic cholinergic synapses are associated with learning and memory, and alterations of those networks may be involved with cognitive decline in normal aging (Potier et al., 2006; also reviewed in Schliebs and Arendt, 2011) and Alzheimer's disease (AD) (Davies and Maloney, 1976; Minger et al., 2000; also reviewed in Penzes et al., 2011). Several lines of research point to a central role for the α7 nAChR in the etiology of AD (Wang et al., 2000; Dineley et al., 2002; Chen et al., 2006; Counts et al.,

*Corresponding author. Tel: +1-402-498-6584; fax: +1-402-498-6351. Barbara.Morley@boystown.org (B. J. Morley).

2007; Dziewczapolski et al., 2009; Hernandez et al., 2010; Heinzen et al., 2010; also reviewed in Bencherif and Lippiello, 2011).

Animal models have identified links between α7 nAChR activity and performance on tasks requiring higher-order cognitive functioning. Blocking α7 nAChRs with the selective antagonist methyllycaconitine (MLA) increased errors in several behavioral tasks (Levin et al., 2002). Intraventricular injection of an antisense oligonucleotide knocked down α7 expression in the hippocampus (42%) and cortex (25%) and impaired performance in the Morris Water Maze (Curzon et al., 2006).

Similarly, results from experiments with α7 nAChR knockout mice have consistently shown that mice carrying the α7 gene deletion have difficulty in performing certain cognitive tasks (Keller et al., 2005; Fernandes et al., 2006; Hoyle et al., 2006; Young et al., 2006, 2011; Brown et al., 2010), most of which require prolonged attention. In an extensive analysis of several behavioral tests, Young et al. (2011) reported that α7 nAChR knockout mice had impaired procedural learning in multiple paradigms, an effect that may be attributable to an attention deficit.

Conversely, the administration of nicotinic agonists generally improves performance. The selective α7 nAChR agonist, PNU-282987, administered before training in the Morris water maze enhanced retention (Vicens et al., 2011; also reviewed in Wallace and Porter, 2011). Nicotine administered in varying doses tends to enhance performance on many learning-related tasks, in part through α7 nAChRs (Levin et al., 2009). Gene delivery of α7 sense DNA into mouse hippocampus increased [3H]MLA binding and temporarily enhanced Morris Water Maze performance in wildtype mice (Ren et al., 2007). Lastly, the administration of the α7 agonist choline reversed the effects of MLA-induced impairment in a dose-dependent manner (Boccia et al., 2010).

We hypothesized that the deletion of the α7 nAChR gene would result in changes in hippocampal dendritic spine density and configuration. We tested the hypothesis by measuring the density of dendritic spines in the basilar and apical tree of the CA1 hippocampal neurons, granule cells and parietal cortex pyramidal neurons. We also quantified dendritic branching in CA1 basilar neurons and in the parietal cortex layer II–III pyramidal neurons.

EXPERIMENTAL PROCEDURES

Animals and tissue preparation

Heterozygote breeders for the α7 knockout mouse strain were purchased from the Jackson Laboratories, and a colony was established at the Boys Town National Research Hospital (BTNRH). The α7 knockout mouse was initially developed and characterized by Orr-Urteger et al. (1997) and Paylor et al. (1998). At the time of acquisition at BTNRH the animals had been backcrossed for eight generations onto the C57Bl/6J background at the Jackson Labs. The colony was further backcrossed at BTNRH after one and 3 years of breeding. The animals used in this study were from the generation backcrossed for a total of 10 generations. The average litter size was 6.9, comparable to the 6.2 average for the C57Bl/6J background strain reported by the Jackson Labs. http://www.informatics.jax.org/external/festing/mouse/docs/C57BL.shtml.

The animals used in this study were from 7 L of heterozygote crosses. Three sets of wildtype and knockout animals were littermates. The remaining two animals in each group were from different litters. They were all housed in groups of 3–4 after weaning in standard mouse cages without any environmental enrichment. Animals were genotyped using the primer

sequences provided by the Jackson Laboratories with conditions optimized in our laboratory. The colony produced wildtype, heterozygote, and knockout animals in the expected proportions. Animals were maintained on a 12:12 light cycle and food and water *ad libitum*.

Five male knockout and five male wildtype animals were sacrificed at 24 days of age (P24) using an overdose (75 mg/ kg) of Nembutal. The brains were rapidly removed and fixed in formalin.

Care and animal use procedures were in strict accordance with the National Institutes of Health Guide for the Care and Use of Animals and were approved by the BTNRH IACUC.

Golgi analysis

Coronal blocks were cut from the fixed tissue containing the hippocampus and overlying Parietal Cortex, and stained using a variant of the rapid Golgi method (Valerde, 1993). Briefly, blocks were impregnated with a solution of osmium tetroxide and potassium dichromate, followed by immersion in silver nitrate; then dehydrated through alcohols and ether–alcohol and embedded in ascending concentrations of low viscosity nitrocellulose. The nitrocellulose was hardened by exposure to chloroform vapors, and affixed to fiber blocks for sectioning on an AO sliding microtome. Coronal sections through the hippocampus and parietal cortex were cut at 120 μm. The sections were through the regions identified by the stereotaxic mouse brain atlas (Franklin and Paxinos, 2008) as −2.18 mm bregma (Fig. 49) and −2.54 mm bregma (Fig. 52). The sections were cleared in alpha-terpineol, rinsed in xylene, placed on slides, and coverslipped under Permount. All slides were coded.

For analysis of dendritic branching, all selected neurons had to meet stringent criteria: the neuron had to be well-impregnated, the branches could not be obscured by other neurons, glia, blood vessels, or other non-descript precipitates. In addition, the soma of the selected neuron had to be located in the middle third of the thickness of the slide. Neurons of the various cell populations that were analyzed meeting all these criteria were randomly selected from the coded slides. For analysis, camera lucida drawings were prepared using Zeiss brightfield research microscopes. The drawings were made using a 40× long-working-distance plan-apochromatic oil-immersion lens, a 1.25× Optivar intermediate lens and a 10× ocular viewer yielding a final magnification of 500×.

Statistical analyses

For the spine counts and dendritic branching, the individual data for each animal were averaged. The average from each animal was considered as one data point. The averages and standard error of the mean (SEM) for each group were calculated and statistical significance was determined using unpaired *t*-tests. The Sholl analyses were conducted using the Wilcoxon rank-sign test.

Dendritic branching of the CA1 basilar tree

Dendritic branching—Dendritic branching was evaluated on the basilar dendritic tree of the CA1 neurons. Camera lucida drawings were prepared of randomly selected neurons from each subject and Sholl analyses were used to assess the amount and distribution of the arbor at increasing distances from the cell body (Sholl, 1953). The branch point analysis was used to determine the complexity of the dendritic arbor.

Sholl analysis—The extent and distribution of neuronal dendritic branching were evaluated by Sholl analysis (Sholl, 1953), whereby a transparent overlay of increasingly

larger concentric circles equivalent to 10-μm intervals is superimposed on the camera lucida drawings. The number of dendritic branch intersections with each progressively larger circle is counted from the soma of each neuron. This generates a profile showing the amount and distribution of dendritic branching material.

Branch point analysis—The complexity of the dendritic tree is also an important phenotypic component of the branching analysis. A bifurcation of a dendritic branch represents a branch point, e.g., when a branch divides into two sub-branches. A first-order branch point is where a primary (first order) branch bifurcates into two second-order branches and so forth. This analysis was based on the number of branch points (bifurcations) of the dendritic arbor and the branch order of the branch points. This depicts both the complexity of the tree (total branch points) and where this complexity is occurring within the tree (lower branch point orders suggest proximal regions of the tree).

Dendritic spines of the CA1 basilar tree

The spines were also analyzed. All visible flanking spines were counted along 30-μm terminal-tip segments of four total segments from each neuron at a magnification of 2000× (100× long working distance objective lens × 2.0 Optivar × 10× eyepiece).

Spine counts—Spines were evaluated from three subjects in each of the two groups. From each hippocampus, three CA1's were randomly selected for spine analysis. For each neuron, spines were analyzed from three basilar segments located on an internal portion of the tree (e.g., not terminal tip segments). From coded slides, all visible flanking spines were counted along 30-μm long segments. A total of nine neurons (27 segments) were counted in each group.

Spine configurations—Based on structural appearance, spines were divided into four categories: Lollipop or L-type (distinct spine head, thin spine neck); Mushroom or M-type (distinct spine head, thickened spine neck, generally shorter than L-type spines; Nubby or N-type spines (poorly defined spine head merging into a thickened spine neck); Dimple or D-type spines (small, no distinct spine head). An example of each structural type is shown in Fig. 2C.

Dendritic spines of the CA1 apical tree

Spine counts—Three internal dendritic segments in the stratum lacunosum–moleculare were evaluated in each randomly selected CA1. As in the basilar dendritic arbor of the CA1, all visible spines were counted along 30-μm segment lengths at a magnification of 2000×. The spine morphology was categorized as described above for the basilar tree.

Parietal cortex layer II–III

Dendritic branching—Dendritic branching was evaluated on the basilar dendritic tree of the layer II–III pyramids. Camera lucida drawings were prepared of randomly selected II–III neurons from each subject and the Sholl analysis was used to assess the amount and distribution of the arbor at increasing distances from the cell body.

Spine counts—Dendritic spines were counted along both internal branch segments and terminal tip segments of the basilar tree of Golgi-stained layer II–III pyramids from the parietal cortex at a magnification of 2000×. Analysis was carried out on five neurons from each of the five subjects in each group (KO and wildtype mice), for a total of 25 neurons in each group… e.g., $N = 5$, $n = 25$.

Granule cells of the dentate gyrus

Dendritic spines were counted along segments of the middle third of the molecular layer of the granule cells at a magnification of 2000×.

RESULTS

Spines of the CA1 basilar tree

A photomicrograph of a mouse hippocampus stained using the Golgi preparation is shown in Fig. 1A. At the bottom of the photomicrograph is a row of hippocampal CA1 neurons. An individual CA1 pyramidal neuron is shown in Fig. 1B. The basilar dendrite is inferior to the soma. An example of a segment from a basilar dendrite is shown in Fig. 2A. Examples of the spine types utilized in this study are shown in Fig. 2C.

Spine counts—The results showed that on the basilar tree, total dendritic spine densities, total spines per neuron, and the density of spines per segment were not different between wildtype and α7 knockout mice and are summarized in Table 1.

Spine counts based on configurations—Thin (L-type) spines were found to be significantly increased (by 64%) in the KO mice on the CA1 basilar tree (unpaired *t*-test, $p < 0.02$; Fig. 3A). Relative to the controls, the knockout mice had significantly fewer dendritic N-type (Nubby) spines (Fig. 3C) but it did not reach statistical significance ($p = .06$). There was not a significant difference in the number of D-type (Fig. 3C) or M-type (Fig. 3D) spines between the knockout and wildtype mice.

Dendritic branching of the CA1 basilar tree

The CA1 basilar dendritic tree had significantly less branching in the regions near the soma in α7 knockout mice in comparison with wildtype animals ($p < .01$ for the first and second branches) (Fig. 4A). The genotypes did not differ in more distal branching, and the knockouts had slightly more branching at branch point 6 (Fig. 4A). The Sholl analysis was significant ($P < .003$, Wilcoxin signed rank test) (Fig. 4B).

Dendritic spines of the apical tree of the CA1 hippocampus

Spine counts—An example of an apical dendrite is shown in Fig. 2B. Based on total brain spine counts ($N = 3$ brains/group), there was a 12% increase in dendritic spines on the apical CA1 tree of the α7 nAChR knockout mice compared to wildtype controls ($p < 0.02$, unpaired *t*-test (Fig. 5A). Based on spines per neuron ($n = 9$ neurons evaluated per group), there was a trend toward significantly more spines on the hippocampal CA1 apical tree of the KO mice ($p = 0.06$, unpaired *t*-test; Fig. 5B).

Spine counts based on configurations—There were no significant differences between knockout and control animals in thin L-type, M-type, or D-type spines (see Table 1).

Dendritic spines on internal branch segments of layer II–III pyramids (basilar tree)

There was no difference in the spine density between the α7 nAChR knockout mice and wildtype controls (Table 1). Although the spine density of the knockout mice showed slightly greater variability, the average number of spines on the internal branch segments was reduced in total by only two percent whether expressed as spines/brain or spines/neuron.

Dendritic spines on terminal tip branch segments of layer II–III pyramids (basilar tree)

Expressed as total spines/subject, there was a slight, but non-significant increase in dendritic spines in the α7 knockout mice (+6%) (Table 1). As seen with the internal branch segments, the KO mice data also had somewhat more variability than the wildtype controls. There was a trend toward total more spines per brain and more spines per neuron in the knockout mice, but neither result was statistically significant (Table 1).

Parietal cortex layer II–III dendritic branching

The Sholl analysis was conducted as shown in Fig. 6. Based on the Sholl analysis, there was significantly less dendritic branching in the knockout mice compared to the wildtype controls ($P < 0.001$) (Fig. 7A). Each data point represents the amount of dendritic material based on the number of "hits" of dendrites crossing a series of enlarging concentric circles originating from the soma. The same data, but expressed as a cumulative total number of "hits" are shown in Fig. 7B.

The knockout mice have 20% less dendritic material in their basilar trees compared to the wildtype controls, but that result was not quite statistically significant ($p = 0.06$, unpaired *t*-test) (Fig. 7C). The cumulative number of hits (representing an estimate of the total dendritic length) expressed for each subject was not statistically significant (Fig. 7D).

The analysis of the complexity of the dendritic tree based on the number of branch points at each of the branch orders was not statistically significant when compared across the entire tree, but it nevertheless showed that the amount of dendritic branching is somewhat less on the first and second branch orders of the dendritic arbor of the knockout mice (Table 1). These are more proximal regions of the arbor, as opposed to the more distal dendritic regions, which appear unaffected by the genotype.

Granule cells of the dentate gyrus

Dendritic spines—Dendritic spines were counted along segments of the middle third of the molecular layer of the granule cells. There was not a significant difference between the wildtype and knockout mice (Table 1). When the same data were expressed for each neuron, there was also no difference in spine density between the wildtype and knockout mice (Table 1).

Dendritic branching—The results of the Sholl analysis from this phase of the study show that there were no significant differences in dendritic branching of the granule cells of the dentate gyrus between the wildtype and the knockout mice (Table 1).

When the data were expressed for each neuron or each subject, the total number of "hits" from the Sholl analysis (=an estimate of the total length of the dendritic branching) showed that for this cell population there is little difference between the controls and the knockout mice (Table 1).

Thus, although there were differences in the amount of dendritic material in a cortical population (e.g., the basilar tree of layer II–III pyramids) there was no effect of the genotype on the granule cells of the hippocampal formation.

There was a non-statistical trend for the more distal portion of the granule cell tree of the knockout mice to have more dendritic branching than the controls. The total number of branch points (=dendritic complexity) is 6% greater in the KO mice compared to the controls (Table 1).

DISCUSSION

Spines on CA1 pyramidal dendrites have been divided into mushroom, thin (L-shaped; lollipop), stubby (Peters and Kaiserman-Abramof, 1970), filopodium (Skoff and Hamburger, 1974), and branched (Sorra et al., 1998). In addition to those reported spine configurations, we also categorized spines as nubby (N-type) and dimple (D-type) in this study. The categorization of the data into spine types was conducted blind to the genotype and was done by qualitative assessment. Spines were not categorized by quantitative measurement.

We observed a highly significant 64% increase in the number of thin (L-type) spines and small decreases in the number of Nubby (N-type), Mushroom (M-type) and Dimple (D-type) on basilar CA1 dendrites. Despite the large difference in the configuration of the spines, the total number of spines/brain or spines/neuron on basilar dendrites was not affected. The data may suggest that thin spines do not mature in the CA1 basilar dendrites or that they are missing requisite inhibitory (GABAergic) input that regulates the plasticity of spine configuration.

Conversely, there was a small but significant increase (+12%) in the number of spines in the apical dendritic tree, but not a difference in spine configuration. There was not a significant difference between wildtype and knockout mice in the number of spines on dendrites in layers II–III of the parietal cortex.

The biological significance of spine morphology and density is controversial. On the basis of studies primarily conducted in cortical regions, it is believed that most mature spines are stable in both number and morphology, but under certain circumstances may undergo considerable change in shape, size, and number (Kirov and Harris, 1999; Grutzendler et al., 2002; Trachtenberg et al., 2002; Holmaat et al., 2005; Majewska et al., 2006; also reviewed in Yuste and Bonhoeffer, 2004; Alvarez and Sabatini, 2007). It has been speculated that spines with large heads are stable and contribute to strong synaptic connections whereas thin spines are motile and unstable and contribute to weak or silent connections (Harris et al., 1992; Kasai et al., 2003; von Bohlen und Halbach, 2009). Thin spines typically have smaller postsynaptic densities (PSDs) that contain N-methyl-D-aspartate (NMDA) receptors but few AMPA receptors (Holmaat et al., 2005; Zuo et al., 2005).

Spine changes selective to the CA1 pyramidal dendrites have been observed in a number of experimental paradigms, suggesting that they are highly susceptible to change after a variety of experimental treatments and may be more plastic than other dendrites. Selective changes or selective responses to drugs have been reported in CA1 basilar dendrites in Alzheimer's disease transgenic mouse models (Wang et al., 2011; Perez-Cruz et al., 2011), aging in C57Bl/6J mice (von Bohlen Und Halbach, 2009), and after spatial learning in wildtype mice (Moser et al., 1997).

The reasons for a larger or selective effect on basal dendrites in α7 knockouts is not immediately obvious, but there are known differences between the inputs to the basal and apical branches of CA1 pyramidal neurons. Although both basal and apical dendrites receive input from CA3 pyramidal cells, basal dendrites receive more input from the Schaffer collaterals (Spruston, 2008). CA3 neurons closer to CA1 project more heavily to basal dendrites (Ishizuka et al., 1990; Li et al., 1994). CA1 basal dendrites have a higher density and different properties of voltage-gated channels than apical dendrites, both of which are important for integrating synaptic inputs (Enoki et al., 2004).

It has been also been suggested (Perez-Cruz et al., 2011) that the GABAergic inhibitory network differentially affects basal dendrites. This hypothesis is consistent with the known differential projections of hippocampal GABAergic interneurons (Klausberger, 2009). A

differential distribution of a subclass of GABAergic interneurons has also been proposed to explain differences between basal and apical dendrites in response to theta pattern stimulation and the resulting long-term potentiation (LTP) (Arai et al., 1994; Haley et al., 1996).

Although the α7 nAChR is widely expressed in the mammalian brain, it is very densely localized on hippocampal interneurons (Freedman et al., 1993; Whiteaker et al., 1999; Fabian-Fine et al., 2001; Adams, 2003). It is well-documented that the α7 nAChR in the hippocampus modulates GABAergic activity (Alkondon et al., 1997; McQuiston and Madison, 1999; Alkondon and Albuquerque, 2001, 2004; Buhler and Dunwiddie, 2001; Kawai et al., 2002; Son and Winzer-Serhan, 2008) and that there are functional consequences in both the developing (Maggi et al., 2004; Liu et al., 2006; Le Magueresse et al., 2006) and adult brain (Campbell et al., 2010).

In the present study we also observed a significant decline in branching in the two most proximal CA1 basilar dendrites ($p < .001$) and to a lesser extent in layer II–III of the parietal cortex, but not in the granule cells of the dentate gyrus. Increased branching in the CA1 neurons has been associated with aging and poorer spatial learning. The decreased branching of the proximal CA1 basal dendrites and parietal cortex dendritic trees observed in the present study may be a compensatory mechanism related to the increase in thin spines.

Recently Lozada et al. (2012) reported that alpha7 knockout mice at age P8 have a deficiency in the number of synapses in the region of the hippocampal CA1 apical dendrite, as assessed by quantitative electron microscopy. The difference was also observed when counting PSD95 and Vesicular Glutamate Transporter immunostained puncta in the same region. A similar deficit with GABAergic synapses (GABA Transporter or $GABA_A$ receptor immunostaining) was not observed. Recordings in hippocampal slices from P12 and P25 mice showed that CA1 pyramidal neurons received less glutamatergic transmission than wildtype controls. The modest increase in the number of CA1 apical spines in our study may reflect an increase in the number of glutamatergic synapses. We did not, however, observe a change in the configuration of apical CA1 spines in alpha7 KO mice, suggesting that chronically increased glutamatergic activity in this region does not necessarily result in a long-term change in spine morphology.

CONCLUSIONS

The results of this study demonstrate that the α7 nAChR knockout mouse exhibits structural changes in the CA1 region of the hippocampus. Spine configuration changes were most pronounced in the basal CA1 basal dendrites. Thin, L-shaped spines were significantly increased while all classes of thick spines were decreased. The results suggest that the absence of α7 nAChRs on GABAergic interneurons may result in the lack of maturation of dendritic spine configuration and/or increased spine plasticity. The observed changes in spine configuration may be related to the attention deficit observed in the performance on α7 knockout mice on learning and memory tasks and may be related to the cognitive prodromal deficits observed in several neurological syndromes, including Alzheimer's disease.

Acknowledgments

This publication was made possible by NIH Grant DC006907 (BJM) and the Nebraska Tobacco Settlement Biomedical Research Foundation (BJM). The authors thank Natalie Meylan, Ashley Cole, and Melissa Casillis for their assistance in generating the microscopic data and Stephanie K. Foley for her help in the statistical analysis of the data. We would also like to acknowledge the Honors College of the University of South Florida for their support in the course of this study.

Abbreviations

AD	Alzheimer's disease
BTNRH	Boys Town National Research Hospital
MLA	methyllycaconitine
nAChR	nicotinic acetylcholine receptor
SEM	standard error of the mean

REFERENCES

Adams CE. Comparison of alpha7 nicotinic acetylcholine receptor development in the hippocampal formation of C3H and DBA/2 mice. Brain Res Dev Brain Res. 2003; 12:137–149.

Alkondon M, Albuquerque EX. Nicotinic acetylcholine receptors α7 and α4β2 subtypes differentially control GABAergic input to CA1 neurons in rat hippocampus. J Neurophysiol. 2001; 86:3043–3055. [PubMed: 11731559]

Alkondon M, Albuquerque EX. The Nicotinic acetylcholine receptor subtypes and their function in the hippocampus and cerebral cortex. Prog Brain Res. 2004; 145:109–120. [PubMed: 14650910]

Alkondon M, Pereira EFR, Barbosa CTF, Albuquerque EX. Neuronal nicotinic acetylcholine receptor activation modulates γ-aminobutyric acid release from CA1 neurons of rat hippocampal slices. J Pharmacol Exp Ther. 1997; 283:1396–1411. [PubMed: 9400016]

Alvarez VA, Sabatini BL. Anatomical and physiological plasticity of dendritic spines. Annu Rev Neurosci. 2007; 30:79–97. [PubMed: 17280523]

Arai A, Black J, Lynch G. Origins of the variations in long-term potentiation between synapses in the basal versus apical dendrites of hippocampal neurons. Hippocampus. 1994; 4:1–9. [PubMed: 8061748]

Bencherif M, Lippiello PM. Alpha7 neuronal nicotinic receptors: the missing link to understanding Alzheimer's etiopathology? Med Hypotheses. 2011; 74:281–285. [PubMed: 19800174]

Boccia MM, Blake MG, Krawczyk MC, Baratti CM. Hippocampal alpha7 nicotinic receptors modulate memory reconsolidation of an inhibitory avoidance task in mice. Neuroscience. 2010; 171:531–543. [PubMed: 20832455]

Brown KL, Cornell DM, De Biasi M, Woodruff-Pak DS. Trace eyeblink conditioning is impaired in α7 but not in β2 nicotinic acetylcholine receptor knockout mice. Front Behav Neurosci. 2010; 4:1–9. [PubMed: 20126432]

Buhler AV, Dunwiddie TV. Regulation of the activity of hippocampal stratum oriens interneurons by α7 nicotinic acetylcholine receptors. Neuroscience. 2001; 106:55–67. [PubMed: 11564416]

Campbell NR, Fernandes CC, Halff AW, Berg DK. Endogenous signaling through α7-containing nicotinic receptors promotes maturation and integration of adultborn neurons in the hippocampus. J Neurosci. 2010; 30:8743–8744.

Chen L, Yamada K, Nabeshima T, Sokabe M. Alpha7 nicotinic acetylcholine receptor as a target to rescue deficit in hippocampal LTP induction in beta-amyloid infused rats. Neuropharmacology. 2006; 50:254–268. [PubMed: 16324726]

Counts SE, He B, Che S, Ikonomovic MD, DeKosky ST, Ginsberg SD, Mufson EJ. Alpha7 nicotinic receptor up-regulation in cholinergic basal forebrain neurons in Alzheimer disease. Arch Neurol. 2007; 64:1771–1776. [PubMed: 18071042]

Curzon P, Anderson DJ, Nikkel AL, Fox GB, Gopalakrishnan M, Decker MW, Bitner RS. Antisense knockdown of the rat alpha7 nicotinic acetylcholine receptor produces spatial memory impairment. Neurosci Lett. 2006; 410:15–19. [PubMed: 17055644]

Davies P, Maloney AJ. Selective loss of central cholinergic neurons in Alzheimer's disease. Lancet. 1976; 2:1403. [PubMed: 63862]

Dineley KT, Xia X, Bui D, Sweatt JD, Zheng H. Accelerated plaque accumulation, associative learning deficits, and up-regulation of alpha7 nicotinic receptor protein in transgenic mice co-

expressing mutant human presenilin I and amyloid precursor proteins. J Biol Chem. 2002; 277:22768–22780. [PubMed: 11912199]

Dziewczapolski G, Glogowski CM, Masliah E, Heinemann SF. Deletion of the alpha7 nicotinic acetylcholine receptor gene improves cognitive deficits and synaptic pathology in a mouse model of Alzheimer's disease. J Neurosci. 2009; 29:8805–8815. [PubMed: 19587288]

Enoki R, Kiuchi T, Koizumi A, Sasaki G, Kudo Y, Miyakawa H. NMDA receptor-mediated depolarizing after-potentials in the basal dendrites of CA1 pyramidal neurons. Neurosci Res. 2004; 48:325–333. [PubMed: 15154678]

Fabian-Fine R, Skehel P, Errington ML, Davies HA, Sher E, Stewart MG, Fine A. Ultrastructural distribution of the alpha7 nicotinic acetylcholine receptor subunit in rat hippocampus. J Neurosci. 2001; 21:7993–8003. [PubMed: 11588172]

Fernandes C, Hoyle E, Dempster E, Schalkwyk LC, Collier DA. Performance deficit of alpha7 nicotinic receptor knockout mice in a delayed matching-to-place task suggests a mild Impairment of working/episodic-like memory. Genes Brain Behav. 2006; 5:433–440. [PubMed: 16923147]

Franklin, KBJ.; Paxinos, G. The mouse brain in stereotaxic coordinates. 3rd ed. New York: Elsevier; 2008.

Freedman R, Wetmore C, Stromberg I, Leonard S, Olson L. α-Bungarotoxin binding to hippocampal interneurons: immunocytochemical characterization and effects on growth factor expression. J Neurosci. 1993; 13:1965–1975. [PubMed: 8478687]

Grutzendler J, Kasthuri N, Gan WB. Long-term dendritic spine stability in the adult cortex. Nature. 2002; 420:812–816. [PubMed: 12490949]

Haley JE, Schaible E, Pavlidis P, Murdock A, Madison DV. Basal and apical synapses of CA1 pyramidal cells employ different LTP induction. Learn Mem. 1996; 3:289–295. [PubMed: 10456098]

Harris KM, Jensen FE, Tsao B. Three-dimensional structure of dendritic spines and synapses in rat hippocampus (CA1) at postnatal day 15 and adult ages: implications for the maturation of synaptic physiology and long-term potentiation. J Neurosci. 1992; 12:2685–2705. [PubMed: 1613552]

Heinzen EL, Need AC, Hayden KM, Chiba-Falek O, Roses AD, Strittmatter WJ, Burke JR, Hulette CM, Welsh-Bohmer KA, Goldstein DB. Genome-wide scan of copy number variation in late-onset Alzheimer's disease. J Alzheimers Dis. 2010; 19:69–77. [PubMed: 20061627]

Hernandez CM, Kayed R, Zheng H, Sweatt JD, Kinele KT. Loss of α7 nicotinic receptors enhances β-amyloid oligomer accumulation, exacerbating early-stage cognitive decline and septohippocampal pathology in mouse model of Alzheimer's disease. J Neurosci. 2010; 30:2442–2453. [PubMed: 20164328]

Holmaat AJGD, Trachtenberg JT, Wilbrecht L, Shepherd GM, Zhang X, Knott GW, Svoboda K. Transient and persistent dendritic spines in the neocortex in vivo. Neuron. 2005; 45:279–291. [PubMed: 15664179]

Hoyle E, Genn RF, Fernandes C, Stolerman IP. Impaired performance of alpha7 nicotinic receptor knockout mice in the five-choice serial reaction time task. Psychopharmacology (Berl). 2006; 189:211–223. [PubMed: 17019565]

Ishizuka N, Weber J, Amaral DG. Organization of intrahippocampal projections originating from CA3 Pyramidal cells in the rat. J Comp Neurol. 1990; 295:580–623. [PubMed: 2358523]

Kasai H, Matsuzaki M, Noguchi J, Yasumatsu N, Nakahara H. Structure-stability-function relationships of dendritic spines. Trends Neurosci. 2003; 26:360–368. [PubMed: 12850432]

Kawai H, Zago W, Berg DK. Nicotinic α7 receptor clusters on hippocampal GABAergic neurons: regulation by synaptic activity and neurotrophins. J Neurosci. 2002; 22:7903–7912. [PubMed: 12223543]

Keller JJ, Keller AB, Bowers BJ, Wehner JM. Performance of alpha7 nicotinic receptor null mutants is impaired in appetitive learning measured in a signaled nose poke task. Behav Brain Res. 2005; 162:143–152. [PubMed: 15922075]

Kirov SA, Harris KM. Dendrites are more spiny on mature hippocampal neurons when synapses are inactivated. Nature. 1999; 2:878–883.

Klausberger T. GABAergic interneurons targeting dendrites of pyramidal cells in the CA1 area of the hippocampus. Eur J Neurosci. 2009; 30:947–957. [PubMed: 19735288]

Le Magueresse C, Safiulina V, Changeux JP, Cherubini E. Nicotinic modulation of network and synaptic transmission in the immature hippocampus investigated with genetically modified mice. J Physiol. 2006; 576:533–546. [PubMed: 16901939]

Levin ED, Bradkey A, Addy N, Siguarani N. Hippocampal alpha7 and alpha4beta2 nicotinic receptors and working memory. Neuroscience. 2002; 109:757–765. [PubMed: 11927157]

Levin ED, Petro A, Rezvani AH, Pollard N, Christopher NC, Strauss M, Avery J, Nicholson J, Rose JE. Nicotinic alpha7 or beta2-containing receptor knockout: effects on radial-arm maze learning and long-term nicotine consumption in mice. Behav Brain Res. 2009; 196:207–213. [PubMed: 18831991]

Li XG, Somogyi P, Ylinen A, Buzsaki G. The hippocampal CA3 network: an *in vivo* intracellular labeling study. J Comp Neurol. 1994; 339:181–208. [PubMed: 8300905]

Liu Z, Neff RA, Berg DK. Sequential interplay of nicotinic and GABAergic signaling guides neuronal development. Science. 2006; 314:1610–1613. [PubMed: 17158331]

Lozada AF, Wang X, Gounko NV, Massey KA, Duan J, Liu Z, Berg DK. Glutamatergic synapse formation is promoted by α7-containing nicotinic acetylcholine receptors. J Neurosci. 2012; 32:7651–7661. [PubMed: 22649244]

Maggi L, Sola E, Minneci F, LeMagueresse C, Changeux JP, Cherubini E. Persistent decrease in synaptic efficacy induced by nicotine at Schaffer collateral-CA1 synapses in the immature rat hippocampus. J Physiol. 2004; 559:863–874. [PubMed: 15272042]

Majewska AK, Newton JR, Sur M. Remodeling of synaptic structure in sensory cortical areas in vivo. J Neurosci. 2006; 26:3021–3029. [PubMed: 16540580]

McQuiston AR, Madison DV. Nicotinic receptor activation excites distinct subtypes of interneurons in the rat hippocampus. J Neurosci. 1999; 19:2887–2896. [PubMed: 10191306]

Minger SL, Esin MM, McDonald B, Keene J, Carter J, Hope T, Francis PT. Cholinergic deficits contribute to behavioral disturbance in patients with dementia. Neurology. 2000; 55:1460–1467. [PubMed: 11094098]

Moser MB, Trommald M, Egeland T, Andersen P. Spatial training in a complex environment and isolation alter the spine distribution differently in rat CA1 pyramidal cells. J Comp Neurol. 1997; 380:373–381. [PubMed: 9087519]

Orr-Urteger A, Goldner FM, Saeiki M, Lorenzo I, Goldberg L, DeBiasi M, Dani JA, Patrick JW, Beaudet AL. Mice deficient in the alpha7 neuronal nicotinic acetylcholine receptor lack alpha-bungarotoxin binding sites and hippocampal fast nicotinic currents. J Neurosci. 1997; 17:9165–9171. [PubMed: 9364063]

Paylor R, Nguyen M, Crawley JS, Patrick J, Beaudet A, Orr-Urteger A. Alpha7 nicotinic receptor subunits are not necessary for hippocampal-dependent learning or sensorimotor gating: a behavioral characterization of Acra7-deficient mice. Learn Mem. 1998; 5:302–316. [PubMed: 10454356]

Penzes P, Cahill ME, Jones KA, VanLeeuwen J-E, Woolfrey KM. Dendritic spine pathology in neuropsychiatric disorders. Nat Neurosci. 2011; 14:285–293. [PubMed: 21346746]

Perez-Cruz C, Nolte MW, van Gaalen MM, Rustay NR, Termont A, Tanghe A, Kirchhoff F, Ebert U. Reduced spine density in specific regions of CA1 pyramidal neurons in two transgenic mouse models of Alzheimer's disease. J Neurosci. 2011; 31:3926–3934. [PubMed: 21389247]

Peters A, Kaiserman-Abramof IR. The small pyramidal neuron of the rat cerebral cortex. The perikaryon, dendrites and spines. Am J Anat. 1970; 127:321–355. [PubMed: 4985058]

Potier B, Jouvenceau A, Epelbaum J, Dutar P. Age-related alterations of GABAergic input to CA1 pyramidal neurons and its control by nicotinic acetylcholine receptors in rat hippocampus. Neuroscience. 2006; 142:187–201. [PubMed: 16890374]

Ren K, Thinschmidt J, Liu J, Ai L, Papke RL, King MA, Hughes JA, Meyer EM. Alpha7 nicotinic receptor gene delivery into mouse hippocampal neurons leads to functional receptor expression, improved spatial memory-related performance, and tau hyperphosphorylation. Neuroscience. 2007; 145:314–322. [PubMed: 17218065]

Schliebs R, Arendt T. The cholinergic system in aging and neuronal degeneration. Behav Brain Res. 2011; 221:555–563. [PubMed: 21145918]

Sholl DA. Dendritic organization in the neurons of the visual and motor cortices of the cat. J Anat. 1953; 87:387–406. [PubMed: 13117757]

Skoff RP, Hamburger V. Fine structure of dendritic and axonal growth cones in embryonic chick spinal cord. J Comp Neurol. 1974; 153:107–147. [PubMed: 4810722]

Son JH, Winzer-Serhan UH. Expression of neuronal nicotinic acetylcholine receptor subunit mRNAs in rat hippocampal GABAergic interneurons. J Comp Neurol. 2008; 511:286–299. [PubMed: 18792073]

Sorra KE, Fiala JC, Harris KM. Critical assessment of the involvement of perforations, spinules, and spine branching in hippocampal synapse formation. J Comp Neurol. 1998; 398:225–240. [PubMed: 9700568]

Spruston N. Pyramidal neurons: dendritic structure and synaptic integration. Nat Rev Neurosci. 2008; 9:206–221. [PubMed: 18270515]

Trachtenberg JT, Chen BE, Knott GW, Feng G, Sanes JR, Welker E, Svoboda K. Long-term in vivo imaging of experience-dependent synaptic plasticity in adult cortex. Nature. 2002; 420:788–794. [PubMed: 12490942]

Valerde F. The rapid Golgi method for staining CNS neurons: light microscopy. Neurosci Protoc. 1993; 1:1–9.

Vicens P, Ribes D, Torrente M, Domingo JL. Behavioral effects of PNU-282987, an alpha7 nicotinic receptor agonist, in mice. Behav Brain Res. 2011:341–348. [PubMed: 20728474]

von Bohlen Und Halbach O. Structure and function of dendritic spines within the hippocampus. Ann Anat. 2009; 191:518–531. [PubMed: 19783417]

Wallace TL, Porter RHP. Targeting the nicotinic alpha7 acetylcholine receptor to enhance cognition in disease. Biochem Pharmacol. 2011; 82:891–892. [PubMed: 21741954]

Wang HY, Lee DH, D'Andrea MR, Peterson PA, Shank RP, Reitz AB. Beta-amyloid (1–42) binds to alpha7 nicotinic acetylcholine receptor with high affinity. Implications for Alzheimer's disease pathology. J Bio Chem. 2000; 275:5626–5632. [PubMed: 10681545]

Wang J, Ono K, Dickstein DL, Arrieta-Cruz I, Zhao W, Qian X, Lamparello A, Subnani R, Ferruzzi M, Pavlides C, Ho L, Hof PR, Teplow DB, Pasinetti GM. Carvedilol as a potential novel agent for the treatment of Alzheimer's disease. Neurobiol Aging. 2011; 32:xx.

Whiteaker P, Davies AR, Marks MJ, Blagbrough I, Potter BV, Wolstenholme AJ, Collins AC, Wonnacott S. An autoradiographic study of the distribution of binding sites for the novel alpha7-selective nicotinic radioligand [3H]-methyllcaconitine in the mouse brain. Eur J Neurosci. 1999; 11:2689–2696. [PubMed: 10457165]

Young JW, Crawford N, Kelly JS, Kerr LE, Marston HM, Spratt C, Finlayson K, Sharkey J. Impaired attention is central to the cognitive deficits observed in alpha7 deficient mice. Eur Neuropharmacol. 2006; 17:145–155.

Young JW, Meves JM, Tarantino IS, Caldwell S, Geyer MA. Delayed procedural learning in α7-nicotinic acetylcholine receptor knockout mice. Genes Brain Behav. 2011; 10:720–733. [PubMed: 21679297]

Yuste R, Bonhoeffer T. Genesis of dendritic spines: insights from ultrastructural and imaging studies. Nat Rev Neurosci. 2004; 5:24–34. [PubMed: 14708001]

Yang G, Zuo Y, Kwon E, Gam W-B. Structure-stability- function relationships of dendritic spines. Trends Neurosci. 2005; 26:360–368.

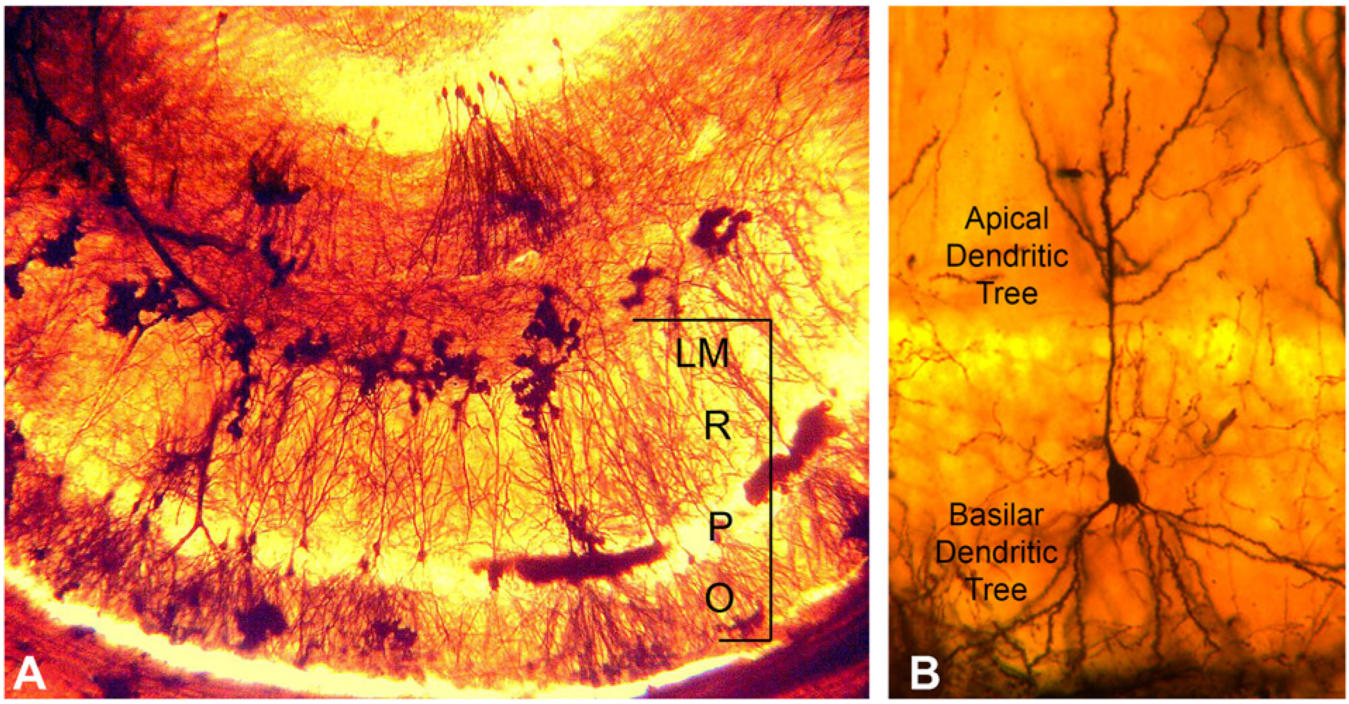

Fig. 1.

The CA1 region of the hippocampus. (A) The CA1 region is marked by the bracket. Stratum oriens (O) is the layer that contains the basal dendritic tree. Stratum pyramidale (P) contains the cell bodies of the pyramidal neurons. Stratum radiatum (R) contains the proximal region of the apical dendritic tree. The most distal part of the apical dendrite is contained in Stratum lacunosum–moleculare (LM). (B) Representative pyramidal cell neuron from our study.

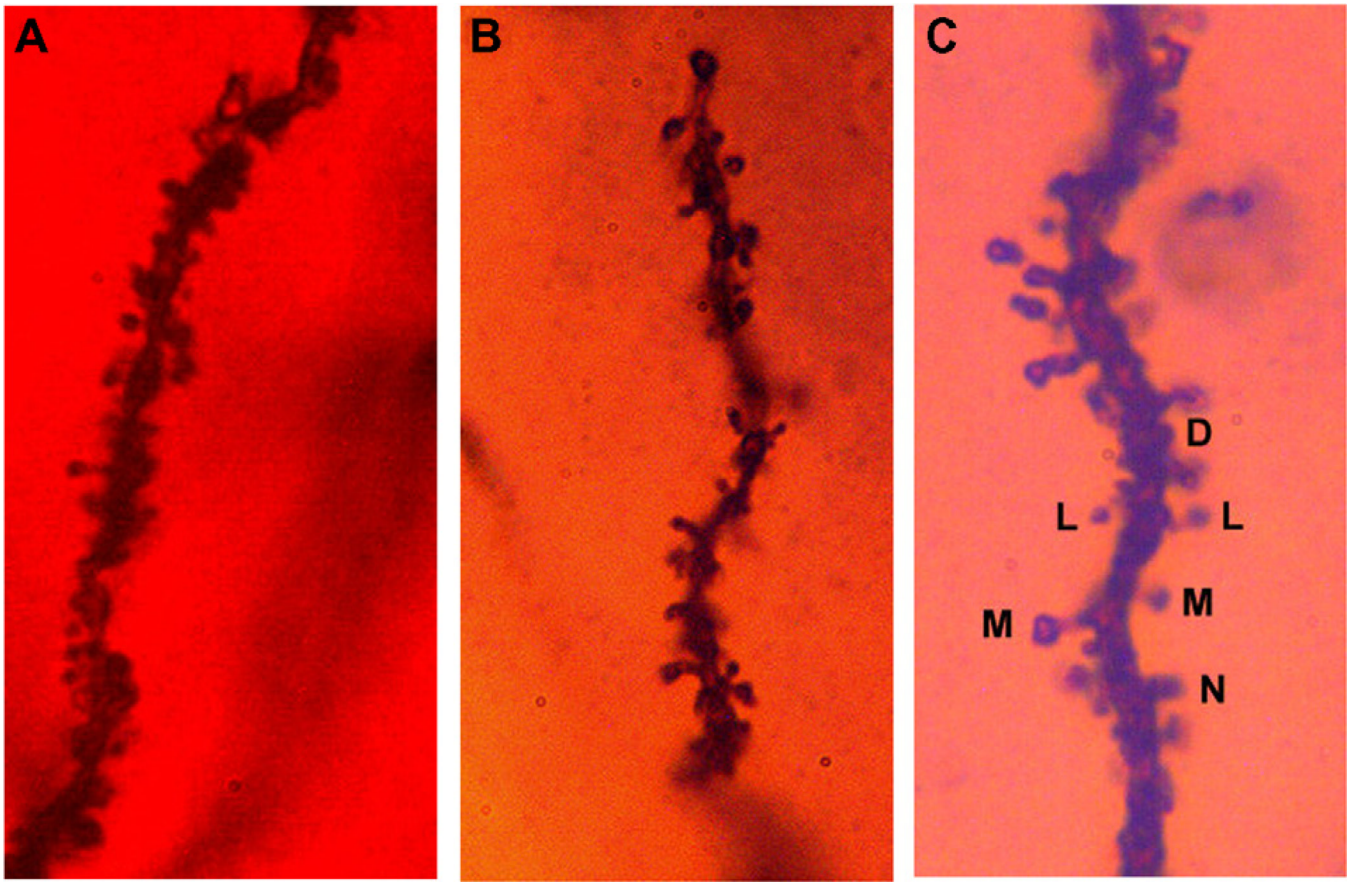

Fig. 2.

(A) Dendritic spines along an internal branch segment of the basilar tree of a CA1 pyramid and (B) dendritic spines along a terminal tip segment from the apical tree of a CA1 pyramid. (C) Dendritic spines were categorized by structural appearance into Lollipop (L); (B) Mushroom (M); (C) Nubby (N); and (D) Dimple (D).

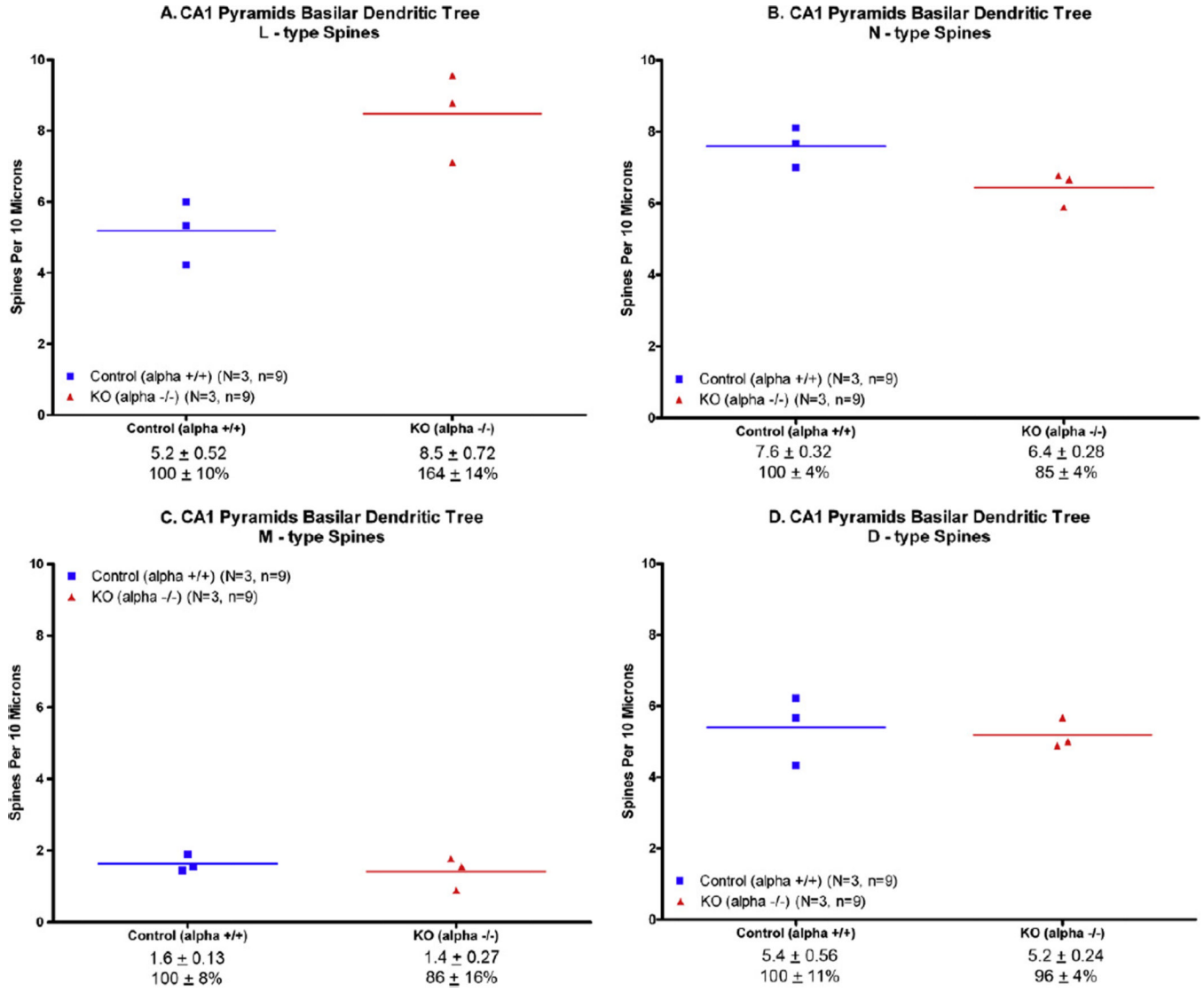

Fig. 3.

Dendritic spines on CA1 basal dendrites were counted as described in the text. The average of each animal is plotted here. The line represents the mean. (A) The largest change was an increase of 64% in the thin (L-type) spine; $p < .01$. (B) The number of N-type spines was decreased by 15%, but did not reach statistical significance ($p = .06$). (C) D-type spine counts were decreased (−14%), but not significantly. (D) Mtype spines were slightly decreased (−4%), but not significantly.

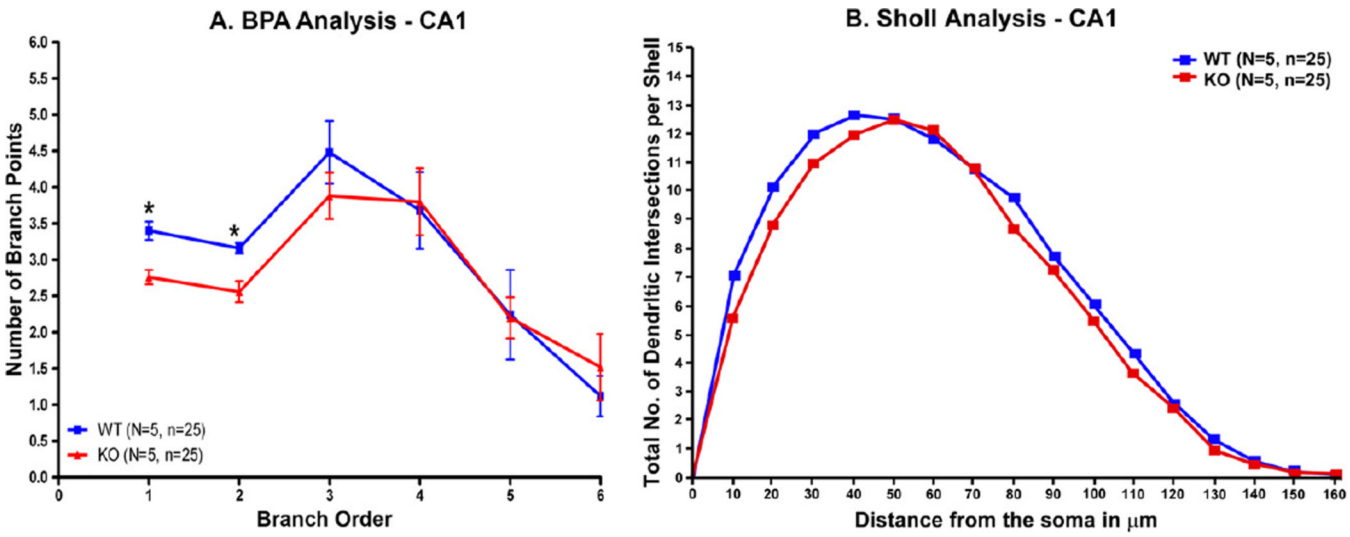

Fig. 4.

Branch point analysis (BPA) of dendritic spines in the basal dendrite was performed as described in the text. (A) The most proximal regions of the basal dendrite in the knockout mice have less branching than wildtype controls (*$P < .01$). (B) The Sholl analysis was highly significant ($P < .003$).

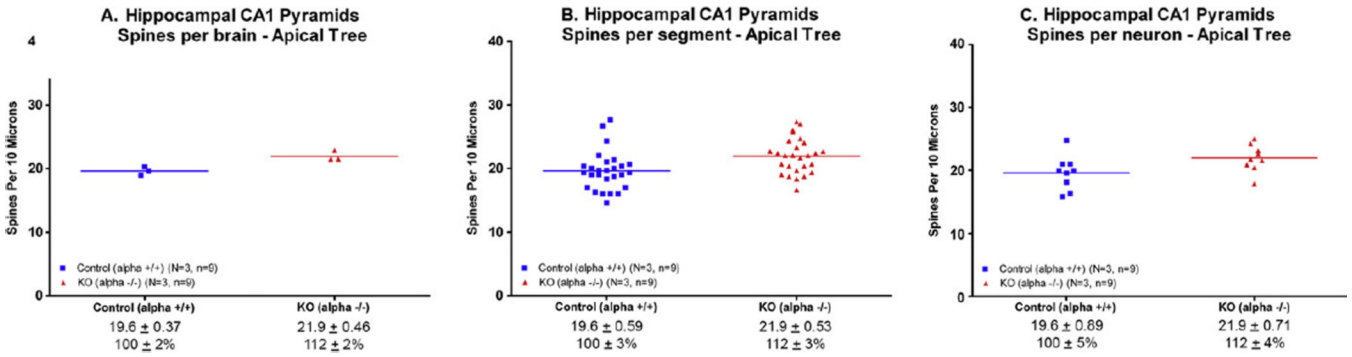

Fig. 5.

The number of dendritic spines in the apical branch of the CA1 pyramidal cell was significantly increased when determined as (A) spines per brain ($p \leq .05$) and (B) spines per segment ($p < .01$), but not (C) spines per neuron ($p = .06$). The line represents the mean.

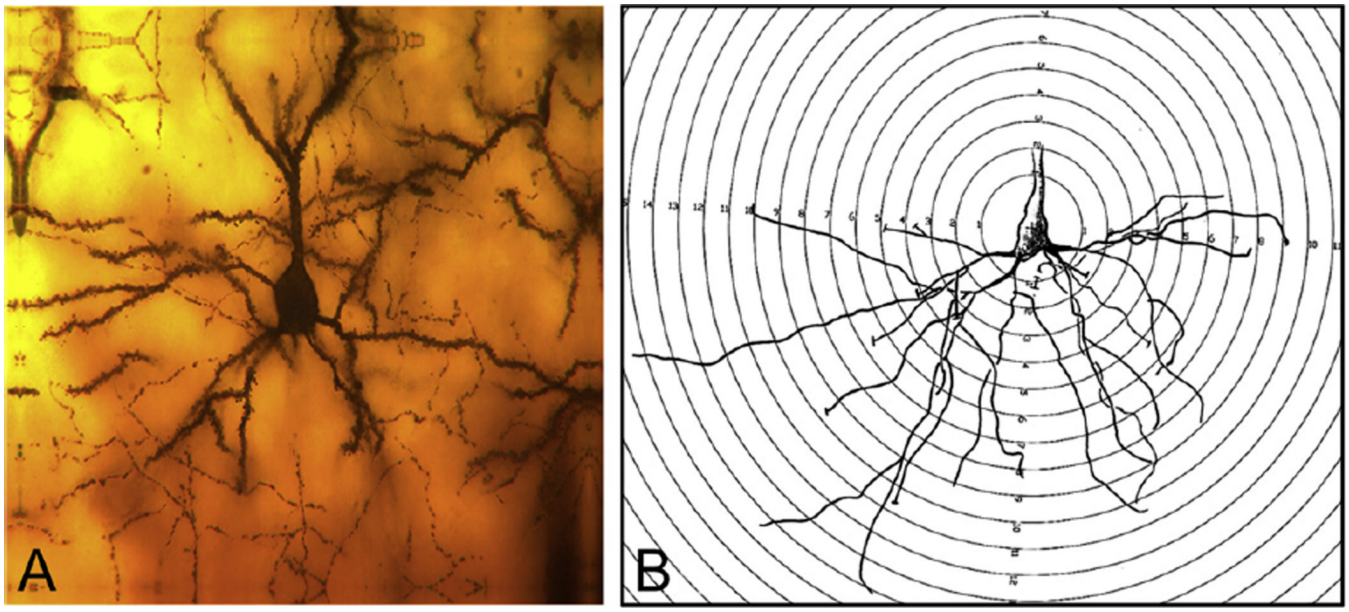

Fig. 6.
The extent and distribution of neuronal dendritic branching in the parietal cortex, layers II–III, were evaluated by Sholl analysis. (A) Typical parietal neuron from our study. (B) Transparent overlay of increasingly larger concentric circles at 10 lm intervals was superimposed on the camera lucida drawings. The number of dendritic branch intersections with each progressively larger circle is counted from the soma of each neuron. This generates a profile showing the amount of dendritic branching material.

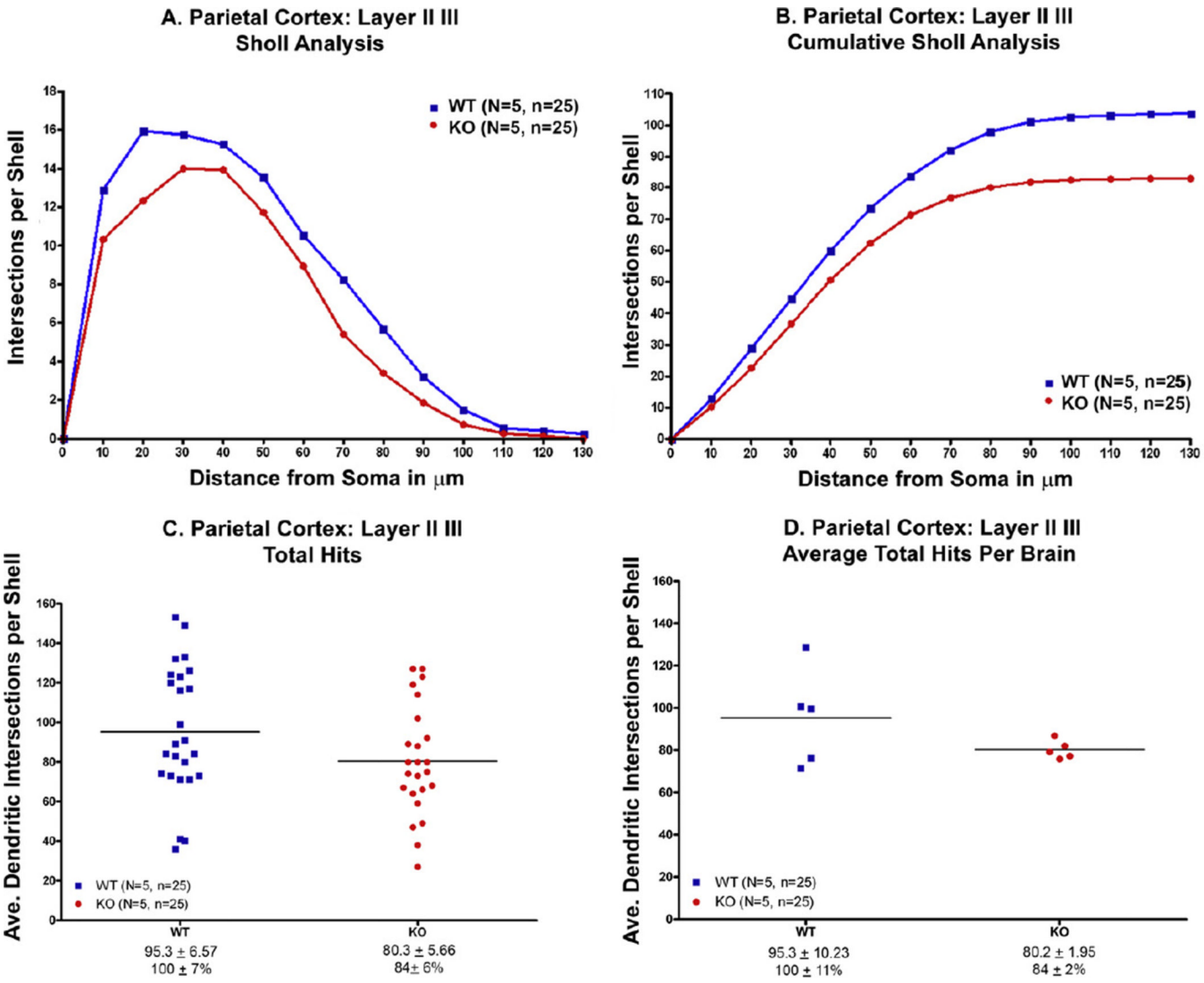

Fig. 7.

(A, B) There was significantly less dendritic branching in the parietal cortex of knockout mice compared to wildtype controls ($p < .001$) using the Sholl analysis. (C) When expressed as the number of "hits" there was less branching but the difference did not reach statistical significance ($p = .06$). (D) When expressed as the average "hits" per brain, the difference did not reach statistical significance ($p = .08$).

Table 1

Summary of non-significant findings

Cell types and measurements	Wildtype (mean ± SEM)	Knockout (mean ± SEM)
CA1 basilar dendrite		
Spines per brain	63.6 ± 1.63	66.5 ± 2.93
Spines per neuron	63.6 ± 1.57	66.5 ± 2.37
Spines per 30 μm segment	63.6 ± 1.19	66.5 ± 1.51
CA1 apical dendrite		
L-type spine density	16.9 ± 1.65	17.9 ± 2.11
M-type spine density	4.7 ± 0.72	5.0 ± 0.56
N-type spine density	19.7 ± 2.17	21.0 ± 1.18
D-type spine density	14.9 ± 1.62	17.9 ± 2.36
Parietal cortex II–III, basilar dendrite		
Spines per brain/internal spines	83.4 ± 2.30	82.4 ± 4.45
Spines per neuron/internal spine	83.4 ± 1.80	83.4 ± 2.76
Spines per brain/terminal tip	69.1 ± 1.92	73.3 ± 4.50
Spines per neuron/terminal tip	69.1 ± 1.53	73.3 ± 2.30
Granule cells		
Spines/brain	5.4 ± 0 .50	5.5 ± 0.17
Spines/neuron	5.3 ± 0.36	5.5 ± 0.19
Sholl analysis: total hits	84.1 ± 4.43	82.5 ± 3.75
Sholl analysis: hits per brain	84.1 ± 6.46	82.6 ± 5.78
Dendritic complexity (branching)	7.6 ± 0.29	8.4 ± 0.23